KSME International Journal, Vol. 18 No. 4, pp. 597~605, 2004

Direct Numerical Simulation of Turbulent Scalar Transport in a Channel with Wall Injection

Yang Na*

Center for Aerospace System Integration Technology, Department of Mechanical Engineering, Konkuk University, Hwayang-dong 1, Gwangjin-gu, Seoul 143-701, Korea

Turbulent temperature field in a channel subject to strong wall injection has been investigated via direct numerical simulation technique. These flows are pertinent to internal flows inside hybrid rocket motors. A simplified model proble m where a regression process at the propellant surface is idealized by wall injection has been investigated to understand how the temperature field is modified. The effect of strong wall injection displaces thermal boundary layer away from the wall and this causes a sharp drop of friction temperature. Turbulent diffusivity and dissipation time scale for temperature field are found to show large variations in the streamwise direction under application of wall blowing. It is, thus, expected that more sophisticated turbulence models would be required to predict the disturbed temperature field accurately.

Key Words: Temperature Field, Wall Injection, Direct Numerical Simulation, Turbulent Diffusivity

Nomenclature

Cp : Specific heat at constant pressure

h : Half channel height

k : Turbulent kinetic energy, $\frac{1}{2}(\overline{u'u'}+\overline{v'v'}+\overline{w'w'})$

L_x, L_z: Domain size in the streamwise and spanwise directions, respectively.

Pr : Molecular Prandtl number

Re_h : Reynolds number based on inlet bulk velocity and half channel height, $U_b h/\nu$

Re_τ : Reynolds number based on inlet friction velocity, $u_{\tau,inlet} h/\nu$

$R_{T'u'}$: $\frac{\overline{T'u'}}{T_{rms}u_{rms}}$

$R_{T'v'}$: $\frac{\overline{T'v'}}{T_{rms}v_{rms}}$

U_b : Bulk velocity at inlet of the computational domain

T_{mean} : Mean temperature

T^+_{mean} : Mean temperature non-dimensionalized by inlet friction temperature, T_{mean}/T_τ

T_{rms} : Rms temperature

T_τ : Friction temperature, $\frac{q_w}{\rho C_p u_\tau}$

t : Time

u_i : Velocity component, $i=1, 23$

u_{rms}, v_{rms}, w_{rms} : Turbulence intensities in x, y and z directions

u_τ : Friction velocity evaluated at inlet of the domain, $\sqrt{\tau_w/\rho}$

x, y, z : Cartesian coordinate in the streamwise, wall-normal and spanwise directions

y^+ : Wall-normal direction normalized by wall unit, $u_\tau y/\nu$

Greek Letters

α_t : Turbulent diffusivity

ε : Wall injection parameter, V_w/U_b

ε_K : Dissipation of velocity fluctuations

ε_T : Dissipation of temperature fluctuations

λ_T : Taylor microscale for temperature, $\sqrt{\frac{1}{\mathrm{Pr}}\frac{\overline{T'T'}}{2}\frac{1}{\varepsilon_T}}$

τ : Time scale of velocity field, k/ε_K

* **E-mail** : yangna@konkuk.ac.kr
TEL : +82-2-450-3467; **FAX** : +82-2-447-5886
Center for Aerospace System Integration Technology, Department of Mechanical Engineering, Konkuk University, Hwayang-dong 1, Gwangjin-gu, Seoul 143-701, Korea. (Manuscript **Received** July 19, 2003; **Revised** January 13, 2004)

τ_T : Time scale of temperature field, $\frac{\overline{T'T'}}{2}/\varepsilon_T$

τ_W : Wall shear stress evaluated at inlet, $\mu\left(\frac{dU}{dy}\right)_{y=0}$

1. Introduction

Better understanding for temperature field for internal flow in a hybrid rocket motor is important for many reasons. Since the stable operation is a design prerequisite for the rocket motor and the occurrence of flow instability carries a potential for serious damage and engine failure, it is important to understand the interaction of internal velocity and temperature fields with regression process. Since the near-wall state of turbulence is likely to be modified by the effect of wall blowing, locally disturbed temperature field is expected to change the local heat transfer characteristics near the propellant surface. The evolution of core flow or large scale motion in the middle of channel will also be strongly influenced by wall injection and thus, an a ccurate prediction of regression and the subsequent combustion processes will be very difficult even if not impossible.

In spite of the importance of these injection driven types of flows such as those in hybrid rocket motors, there has been significantly less effort both in experimental and turbulence modeling studies than in other common shear flows. Most of previous studies (Williams et al., 1969; Beddini, 1986; Traineau et al., 1986; Dunlap et al., 1990; Liou and Lien, 1995) have dealt with very weak blowing and Lee et al.(2003), analyzed the combustion instability occurring in the hybrid rocket motor but none of them investigated turbulent temperature field. This fact is reflected in a difficulty of predicting the temperature field using currently available turbulence models with satisf actory accuracy.

The present work is motivated by the need for the high quality data on the temperature statistics of turbulent flows influenced by strong wall-injection in order to understand how the temperature field is modified and to support RANS and LES modeling developments. For this purpose, a method of direct numerical simulation was chosen for the present study. Since the details of the velocity field were already explored in the first part of this research (Na, 2003), the results regarding temperature field will be mainly discussed here.

2. Numerical Methodology

2.1 Governing equations

A very simplified yet sufficiently realistic model problem has been considered to enable DNS and, at the same time, to serve for the purpose of the present work. The flow configuration is shown schematically in Fig. 1. A regression process at the propellant surface is idealized by wall injection. The streamwise extent of a domain is $L_x=26h$, the spanwise extent is $L_z=6.5h$ where h is the half channel height. In terms of wall units (based the friction velocity at inlet of the domain), the domain size is roughly equivalent to 3820, 294, 955 in the streamwise, wall-normal and spanwise directions, respectively and a length of about 1900 wall units is allowed for the injection-driven flow regime. By referencing to most of the available DNS results (Kasagi and Shikazono, 1995; Kim et al., 1987; Na et al., 1999), it is thought that the choice of about 1900 wall unit is generally reasonable in capturing the characteristics of the injection-driven flow.

Since the Mach number in the hybrid motor is in general less than 0.1, the following non-dimensionalized governing equations for velocity

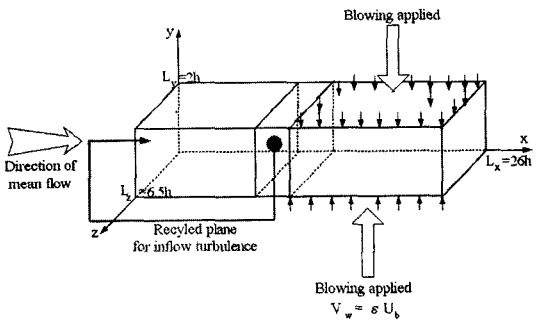

Fig. 1 Flow configuration

and temperature fields of unsteady incompressible viscous flows are solved on a rectangular staggered grid (Harlow and Welch, 1965).

$$\frac{\partial u_i^*}{\partial x_i^*}=0 \tag{1}$$

$$\frac{\partial u_i^*}{\partial t^*}+\frac{\partial}{\partial x_j^*}(u_i^* u_j^*)=-\frac{\partial p^*}{\partial x_i^*}+\frac{1}{Re_h}\frac{\partial^2 u_i^*}{\partial x_j^* x_j^*} \tag{2}$$

$$\frac{\partial T^*}{\partial t^*}+\frac{\partial}{\partial x_j^*}(u_j^* T^*)=\frac{1}{Re_h \mathrm{Pr}}\frac{\partial^2 T^*}{\partial x_j^* x_j^*} \tag{3}$$

All the variables are made dimensionless using an inlet bulk velocity, upper wall temperature and a half-channel height. The superscript * will be dropped hereinafter for convenience. It is assumed that the fluid density is independent of temperature so that the heat is essentially transported as a passive scalar, without producing buoyant force.

The governing Eqns. (1)-(3) are integrated in time using a semi-implicit scheme. A low-storage three-substep, third order Runge-Kutta scheme (Spalart et al., 1991) is used for treating convective terms explicitly and a second order Crank-Nicolson scheme for viscous terms semi-implicitly. All the spatial derivatives are approximated with second order central difference scheme except for the convection term in Eq. (3). It has been reported that the central differencing applied to convection terms in the passive-scalar equation with inflow-outflow boundary condition led to numerical instability (Akselvoll and Moin, 1996) and thus, widely used QUICK scheme (Leonard, 1979) was incorporated as a remedy for the present work.

2.2 Boundary conditions

Wall injection starts from $x/h=13.4$ along both upper and lower walls. The strength of wall-injection is denoted by $\varepsilon=V_w/U_b$, where V_w is the strength of injection applied in the normal directiont the wall and U_b is the bulk velocity at inlet of the domain. In the present study, the value of $\varepsilon=0.05$ is chosen to investigate the effect of strong wall injection.

The no-slip boundary is used along the wall except in a region where constant blowing is applied ($x/h>13.4$). The bottom wall is cooled and the top wall is assumed to be heated at the same rate so that both walls are maintained at constant temperature ($-T_w$ and T_w respectively). The flow is assumed to be homogeneous in the spanwise direction, justifying the use of periodic boundary conditions in that direction.

A popular convective boundary condition, which allows the turbulent structures generated inside the domain to leave smoothly, is used for the outflow boundary condition. In order to generate a turbulent inlet condition as a function of time, a periodic channel is attached in front of the domain where the injection is applied.

2.3 Computational details

The Reynolds number, $U_b h/v$ is set to 2250 and is approximately equivalent to $Re_\tau \approx 150$ when the inlet friction velocity is used. The Prandtl number is set to 1 (Pr=1).

Computations are conducted with two different resolutions in order to see the resolution effect on $257\times129\times129$ and $513\times257\times129$ grids but only the results with $513\times257\times129$ grids will be presented here otherwise indicated. The $513\times257\times129$ grid system gives the grid resolution of approximately $\Delta x^+\approx7.5$, $\Delta y^+_{\min}\approx0.0055$, $\Delta y^+_{\max}\approx1.8$, $\Delta z^+\approx7.5$ using wall variables defined at inlet of the domain. Judging from the previous work on channel flow by the spectral method by Na et al.(1999) and Miyauchi and Tanahashi's turbulent mixing layer simulation (1993), the resolution chosen in the present study is better in both of regions with and without wall-injection.

For the calculation of statistical quantities, averages are performed over the homogeneous spanwise direction and time and hence, single-point statistics are functions of both x and y. In the present flow configuration, the flow experiences complex changes after the injection is applied and this causes slower statistical convergence than in the upstream. The total averaging time is 60 h/U_b.

Figures 2(a)-(b) show the effect of resolution on the mean and rms temperatures in a plain channel region. Essentially the flow in this region

should be that of simple channel flow in a statistical mean sense. For a proper comparison, the results from the present simulations taken at $x/h=1.0$ are compared with those of Na et al. (1999) obtained with a pseudo-spectral method. Since the different resolution tends to make the difference in friction temperature (as well as friction velocity), the direct comparison of T^+_{mean} instead of T/T_w would be a more severe test. The mean temperature profile shows that the current resolution is generally good enough to predict the first order temperature statistics. Figure 2(b) indicates that the higher resolution improves the prediction of rms values but the present results are consistently lower near the local maximum point around $y^+\approx 17$ and consistently higher in the middle of the channel than those obtained from a pseudo spectral method. One of the possible reason is the damping caused by the QUICK scheme. Especially, the temperature gradient is larger in a region near the wall, it is expected that the larger production of $\overline{T'T'}$ and temperature dissipation occur locally here. Thus, the scheme which is dissipative in nature is likely to under-predict the temperature fluctuation. The truncation error resulting from a second order finite differencing can be another reason for the discrepancy shown in Fig. 2(b).

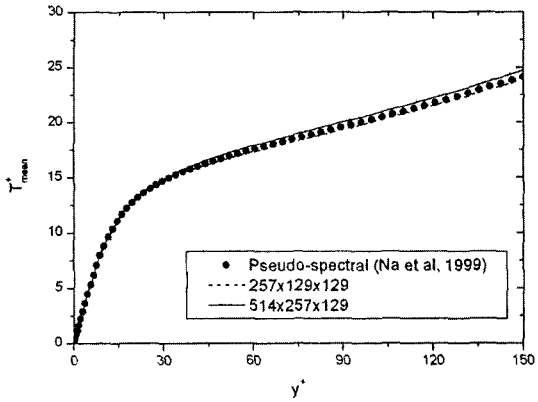

(a) T^+_{mean} vs. y^+

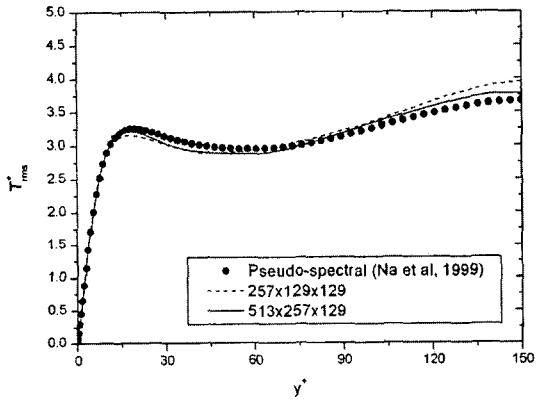

(b) T^+_{rms} vs. y^+

Fig. 2 Comparison of temperature statistics

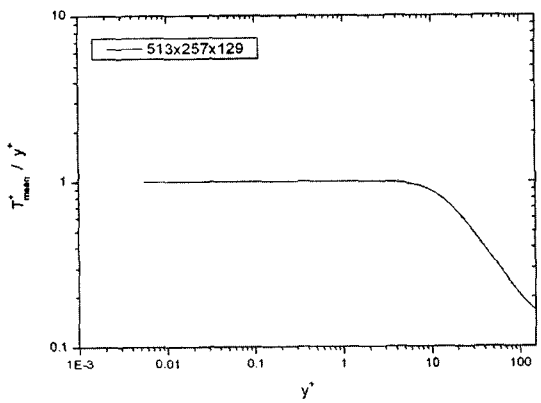

Fig. 3 Limiting behavior of mean temperature in semi-log coordinate, where T^+_{mean} is normalized by y^+

Figure 3 shows the limiting behavior of mean temperature divided by the dimensionless distance from the wall. A conductive sublayer, where a relation $\overline{T}^+=\mathrm{Pr}y^+$ should hold, is clearly seen and the limiting value for $\overline{T}^+/y^+$ as $y^+\to 0$ is found to be 1.0003. This result along with Figs. (2) suggests that the present resolution for the temperature field is sufficient for the purpose of the paper.

3. Results

The flow experiences strong streamwise acceleration or inhomogeneity due to the effect of wall injection. In addition to the complex flow elements in the middle of the channel, the effect of blowing creates totally displaced thermal boundary layer away from the wall. Friction temperature, $T_\tau=\frac{q_w}{\rho C_p u_\tau}$ shown in Fig. 4 indicates that the conduction heat transfer (or

equivalently, temperature gradient) at the wall actually decays faster than the friction velocity. This result provides a basis for assuming that the hydrodynamic and thermal boundary layers react to strong injection of different extents.

The progression of mean temperature profiles shown in Fig. 5 suggest that the temperature profiles deviate significantly from that of non-transpired channel flow (Na et al., 1999). Especially after the downstream of $x/h=15.1$, temperature gradient at the wall almost vanishes and this causes very low heat transfer rate to the flow.

Temperature fluctuations are presented in Fig. 6. Since the mean flow dynamics in the present configuration are significantly different from those in non-transpired channel, the distributions of temperature fluctuation show sizable departure as well. The locations of maximum intensity progressively move away from the wall as the flow goes through a region of wall injection. In order to see how the wall injection influences the fluctuating velocity and temperature fields, streamwise velocity intensities at several streamwise locations are shown in Fig. 7. It is compared with T_{rms} given in Fig. 6. The impact of the injected vertical flow upon the turbulent boundary layer is accompanied by the lifted shear layer and the interaction of the boundary layer with the injection induces different flow characteristics for the cases of streamwise velocity and temperature. In other words, the maximum of u_{rms} appears closer to the wall than that

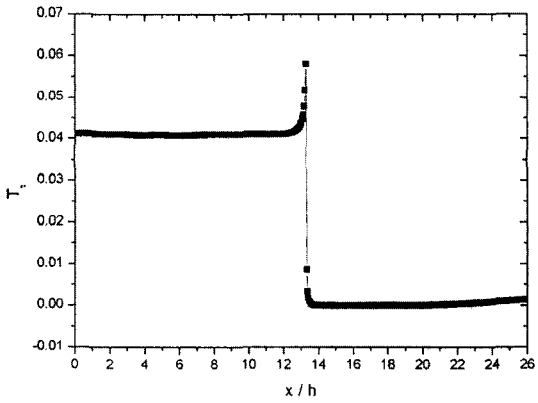

Fig. 4 Distribution of friction temperature, $T_\tau=\frac{q_w}{\rho C_p u_\tau}$

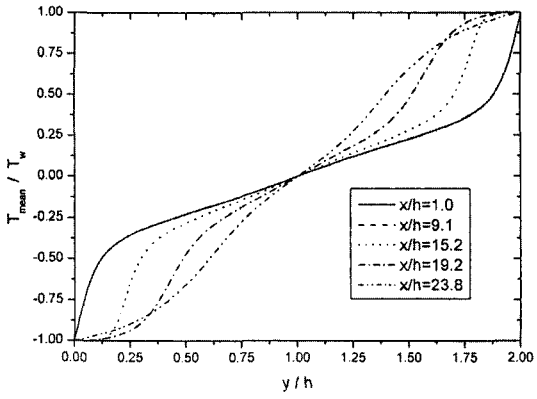

Fig. 5 Profiles of mean temperature at several streamwise locations

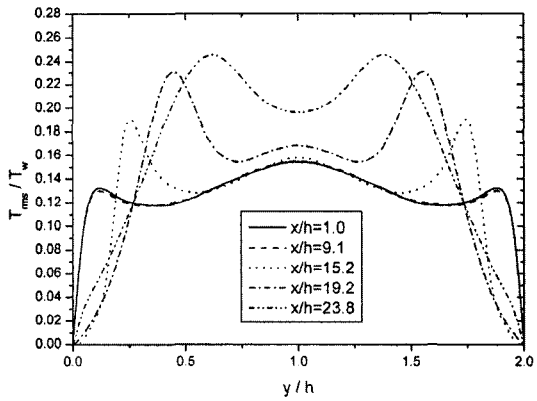

Fig. 6 Profiles of temperature fluctuation at several streamwise locations

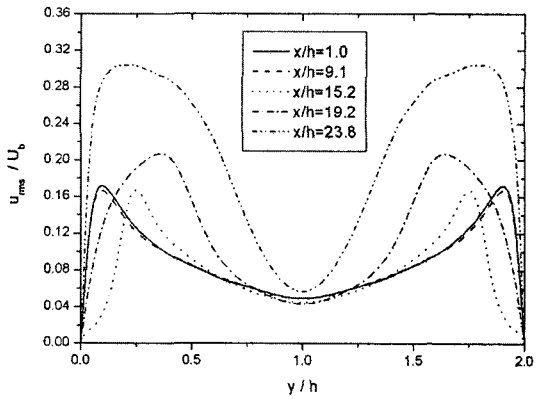

Fig. 7 Profiles of streamwise velocity intensity, u_{rms}, at several streamwise locations

of T_{rms}. As found in Fig. 4, the thermal boundary layer is pushed further away from the wall than the hydrodynamic boundary layer by the action of wall injection and naturally most of the temperature statistics are skewed to the middle of the channel. Also, the temperature boundary condition generates the finite temperature gradient in the middle of the channel as opposed to the velocity gradient and this results in a finite temperature fluctuation there.

Reynolds shear stress $(-\overline{u'v'})$ as well as turbulent vertical heat flux $(-\overline{T'v'})$ are compared in Fig. 8. These quantities are directly related to turbulent transport of momentum and heat respectively, and are subject to crowded attention for RANS type modelling. As the flow goes through a region of higher pressure gradient induced by the wall injection, both Reynolds shear stress and turbulent vertical heat flux exhibit broader region of high transport.

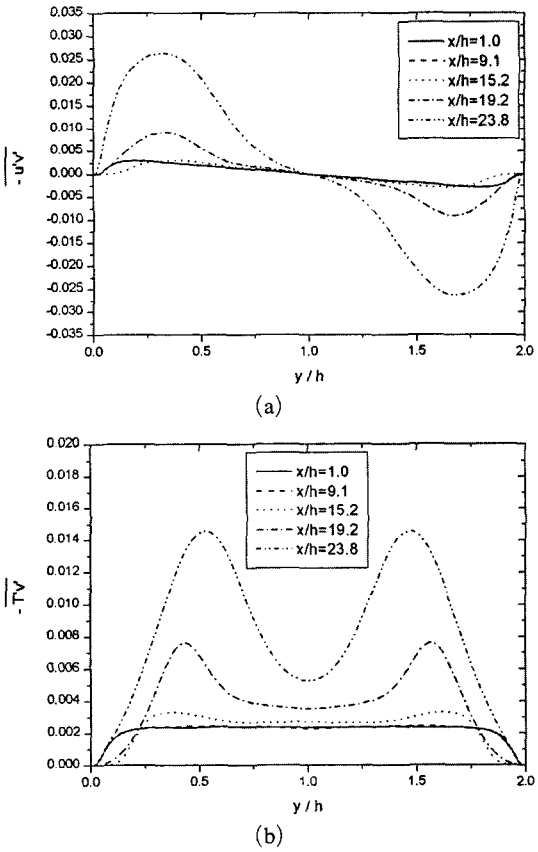

Fig. 8 (a) Profiles of Reynolds shear stress, $-\overline{u'v'}$
(b) Profiles of turbulent heat flux, $-\overline{T'v'}$

Using $\overline{T'v'}$, one can calculate the turbulent diffusivity shown in Fig. 9 at several streamwise locations. Significant variation of turbulent diffusivity with x can be realizable and it is clear that the near-wall RANS modeling problem should be very different from that of non-transpired walls. At $x/h=15.1$, α_t remains small up to $y/h<0.25$ mainly due to the vanishingly small $\overline{T'v'}$ at this location. For $x/h>15.1$ turbulent diffusivity increases abruptly as the flow moves downstream. From a modeling point of view, turbulent diffusivity is assumed to be proportional to the turbulence time-scale times the velocity-scale squared (usually given by a turbulent kinetic energy). In this context, a sudden increase of turbulent kinetic energy (Na, 2003) is more responsible for sudden increase of turbulent diffusivity because the time-scale actually decreases as will be discussed later in Fig. 13.

The behavior of the two different correlation coefficients $R_{Tu}=\dfrac{\overline{T'u'}}{T_{rms}u_{rms}}$ and $R_{Tv}=\dfrac{\overline{T'u'}}{T_{rms}v_{rms}}$ are illustrated in Figs. 10(a)-(b). Again, strong variations with x of these correlations are noticeable. Especially, the correlation between T and u in the vicinity of the wall has been dropped significantly and this is another evidence that the analogy between streamwise velocity and temperature does not hold for the case of strong injection. By looking at the governing Eqns. (2)-(3), the noticeable difference in streamwise velocity

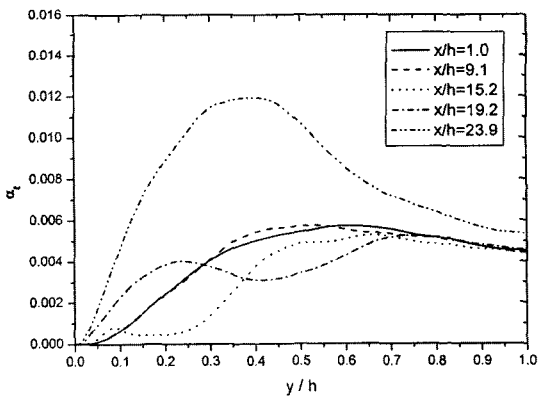

Fig. 9 Profiles of turbulent diffusivity, α_t

and temperature can be created by the pressure gradient term. For $x/h=15.2$, which is located near downstream of the initiation point of wall injection, the flow experiences a sudden change of pressure gradient and this location shows a negligible correlation. Further downstream, the correlations show a sign of recovering to that of non-transpired wall.

The variation of temperature dissipation, ε_T is plotted in Fig. 11. In a region without wall injection, the maximum dissipation occurs at the wall. But with the initiation of wall injection, the maximum point starts to progressively move away from the wall. This behavior can be explained by looking at the behavior of mean temperature profiles shown in Fig. 5. A region of large temperature gradient in the wall-normal direction generally corresponds to a region of large temperature dissipation and fluctuations. As shown earlier, the thermal boundary layers are lifted due to a strong wall injection and this causes a larger temperature gradient and, thus, a larger dissipation to occur away from the wall. The sum of integrated (over y) temperature dissipation increases and a region of non-negligible dissipation becomes wider with x. This is likely to be related to the prevalent shear layer generated by the application of wall injection.

One can use ε_T to define a micro-scale, analogous to that defined by Taylor for dissipation of turbulent energy, $\lambda_T^2=\frac{1}{\mathrm{Pr}}\frac{\overline{T'T'}}{2}\frac{1}{\varepsilon_T}$. Figure 12 presents the distribution of λ_T at several streamwise locations. It is found that λ_T decreases in

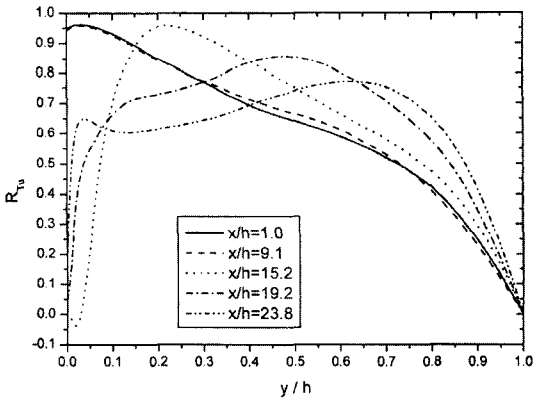

(a) $R_{Tu'}=-\dfrac{\overline{T'u'}}{T_{rms}u_{rms}}$

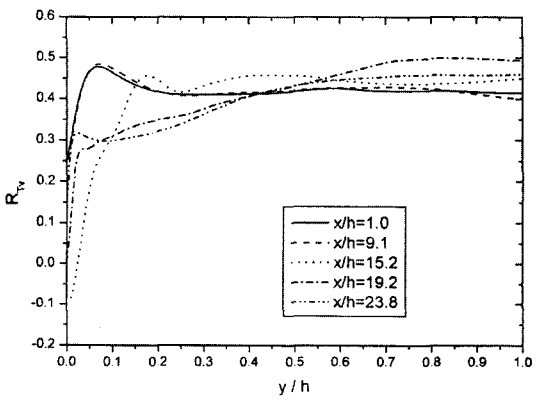

(b) $R_{Tv'}=-\dfrac{\overline{T'v'}}{T_{rms}v_{rms}}$

Fig. 10 Profiles of correlation coefficients

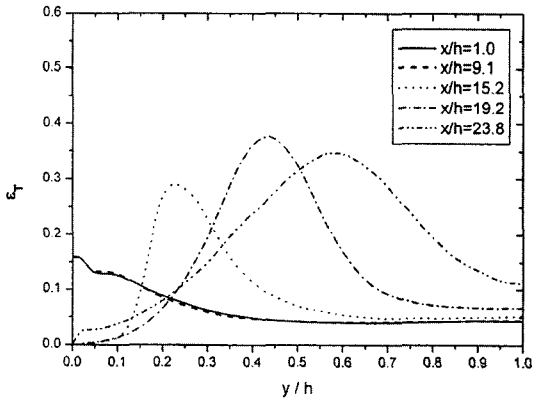

Fig. 11 Distribution of temperature dissipation, ε_T

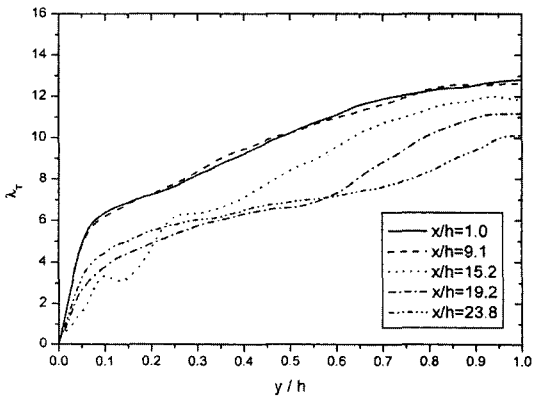

Fig. 12 Distribution of Taylor micro-scale for temperature, λ_T

a region of wall injection. This result suggests that the contribution of high wave numbers becomes more important with increasing x.

A base of $k-\varepsilon$ and Reynolds stress closure models is the definition of a characteristic time scale, τ, which is calculated as $\tau=k/\varepsilon$. In the conventional $k-\varepsilon$ model, the turbulent viscosity is taken as $\nu_t \sim k\tau \sim k^2/\varepsilon$. Similarly, in an attempt to model α_t, another time scale τ_T has been widely used, which is defined as $\alpha_t \sim k\tau_T$. Nagano and Kim (1988) made assumptions that $\alpha_t \sim k\tau_T$ or $\alpha_t \sim k(\tau_T\tau)^{1/2}$. Calculated time scale τ_T at several streamwise locations are presented in Fig. 13. The significant variation with x suggests that the principal theoretical problem to relate the temperature fluctuations to the properties of the fluctuating velocity will not be a minor work and a critical test for the models of scalar-transport will be their ability to predict the influence of wall injection on various temperature statistics shown in the present work.

In earlier study (Na, 2003), it was shown that the Reynolds stress term was an order of magnitude smaller than any other terms in the mean momentum equation budget in the region of wall injection. But in the absence of pressure gradient term, the Reynold stransport term is not negligible and is in balance with the convective term in the mean temperature equation budget. Thus, the conjecture that the prediction of mean flow alone will not be very sensitive regardless of turbulence models used since the mean flow is not strongly influenced by the turbulence and also does not appear to hold for the prediction of temperature field.

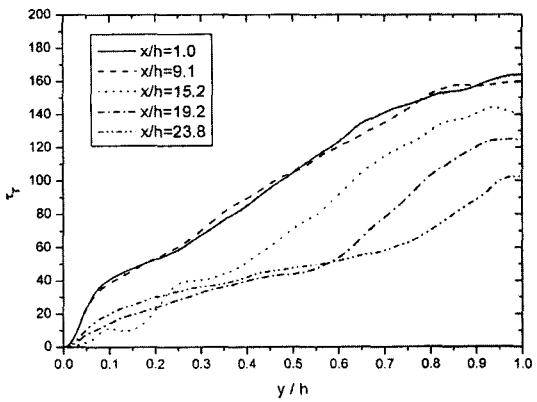

Fig. 13 Distribution of dissipation time scale for temperature, τ_T

4. Summary

The effect of strong wall-injection on temperature field has been investigated using a DNS technique in the injection-driven internal flow and various statistical quantities on temperature field were reported. The complexity of the flow comes from the interaction of mean flow with strongly injected normal flow at the wall and the subsequent evolution of the flow is characterized by a non-negligible streamwise inhomogeneity.

A rapid drop of friction temperature can be explained by the fact that the velocity and temperature fields respond to the wall injection to a different degree. This behavior will raise an issue that low heat transfer rate near the propellant surface influences the regression process in an adverse manner.

The classical approach in turbulent scalar transport study is to use the analogy which assumes that the turbulent diffusivity is proportional to the turbulent viscosity. Although the present results indicate that $R_{t'v'}$ and turbulent diffusivity are not correlated with $R_{u'v'}$ and turbulent viscosity in a simple manner. This fact in addition to the findings that the dissipation time scale for temperature field decays rapidly would imply that the most of the current turbulence models tuned for non-transpired walls are not expected to work equally well for the strong-injection driven flow.

Acknowledgment

This research was supported by the Agency for Defense Development under the contract UD010006AD.

References

Akselvoll, K. and Moin, P., 1996, "Large Eddy Simulation of Turbulent Confined Coannular Jets and Turbulent Flow Over a Backward Fac-

ing Step," Rep. TF-63, Thermoscience Division, Dept. of Mechanical Eng., Stanford University.

Beddini, R. A., 1986, "Injection-Induced Flows in Porous Walled Ducts," *AIAA J.*, Vol. 24, No. 11, pp. 1766~1773.

Dunlap, R., Blackner, A. M., Waugh, R. C. Brown, R. S. and Willoughby, P. G., 1990, "Internal Flow Field Studies in a Simulated Cylindrical Port Rocket Chamber," *J. Prop. Power*, Vol. 6, No. 6, pp. 690~704.

Harlow, F. H. and Welch, J. E., 1965, "Numerical Calculation of Time Dependent Viscous Incompressible Flow of Fluid with Free Surface," *Phys. Fluids*, Vol. 8, pp. 2182~2189.

Kasagi, N. and Shikazono, N., 1995, "Contribution of Direct Numerical Simulation to Understanding and Modeling Turbulent Transport," *Proc. R. Soc. Lond. A.*, Vol. 45, pp. 257~292.

Kim J., Moin, P. and Moser, R., 1989, "Turbulence Statistics in Fully Developed Channel Flow at Low Reynolds Number," *J. Fluid Mech.*, Vol. 177, pp. 133~166.

Lee, C., Lee, J. and Byun, D., 2003, "Transient Analysis of Hybrid Rocket Combustion by the Zeldovich-Novozhilov Method," *KSME Int. J.*, Vol. 17, No. 10, pp. 1572~1582.

Liou, T. M. and Lien, W. Y., 1995, "Numerical Simulations of Injection-Driven Flows in a Two Dimensional Nozzleless Solid Rocket Motor," *J. Prop. Power*, Vol. 11, No. 4, pp. 600~606.

Lund, T., Wu, X. and Squires, K., 1998, "Generation of Turbulent Inflow Data for Spatially Developing Boundary Layer Simulation," *J. Comput. Physics*, Vol. 140, pp. 233~258.

Miyauchi, T. and Tanahashi, M., 1993, "Test case : Temporally Developing Chemically Reacting Turbulent Mixing Layer," http ://www. thtlab.t.u-tokyo.ac.jp .

Na, Y., Papavassiliou, D. V. and Hanratty, T., 1999, "Use of Direct Numerical Simulation to Study the Effect of Prandtl Number on Temperature Fields," *Int. J. Heat and Fluid Flow*, Vol. 20, pp. 187~195.

Na, Y., 2003, "Direct Numerical Simulation of Channel Flow with Wall Injection," *KSME Int. J.*, Vol. 17, No. 10, pp. 1543~1551.

Nagano, Y. and Kim, C., 1988, "A Two-Equation Model for Heat Transport in Wall Turbulent Shear Flow," *J. Heat Trans.*, Vol. 100, pp. 583~589.

Leonard, B. P., 1979, "A Stable and Accurate Convective Modeling Procedure Based on Quadratic Upstream Interpolation," *Comput. Methods Appl. Mech. Eng.*, Vol. 19, p. 59.

Spalart, P. R., Moser, R. D. and Rogers, M., 1991, "Spectral Methods for the Navier-Stokes Equations with One Infinite and Two Periodic Directions," *J. Comput. Phys.*, Vol. 96, pp. 297~324.

Traineau, J. -C., Hervat, P. and Kuentzmann, P., 1986, "Cold Flow Simulations of a Two Dimensional Nozzleless Rocket Motor," Tech. Rep. 86-1447. AIAA.

Williams, F. A., Barrere, M. and Huang, N. C. 1969, "Fundamental Aspects of Solid Propellant Rockets," NATO AGARDograph, No. 16.